PREPARATION AND CHARACTERIZATION OF COPPER SUBSTITUTED MAGNESIUM-ZINC FERRITES

San Htar Oo[1], Aye Aye Lwin[2], Zune Hnin Pwint[3] and Win Kyaw[4]

Abstract

A series of Copper substituted Magnesium-Zinc ferrites, $Mg_{0.5}Zn_{0.5-x}Cu_xFe_2O_4$ (where x = 0.0 – 0.5 with the step of 0.1) were prepared by solid state reaction method. Stoichiometric compositions of MgO, ZnO, CuO and Fe_2O_3 were used. XRD patterns indicated that the samples were cubic structure and the crystallite sizes were estimated by using the observed XRD spectral lines. Microstructural properties of the samples were investigated by Scanning Electron Microscope (SEM). It was found that the grain sizes of the samples depend on the concentration of Cu. Some pores were found in the observed SEM images. Vibrational characteristics of the samples were investigated by Fourier Transform Infrared (FTIR) spectroscopic method. The collected spectral lines were identified by using molecular vibrational theory and standard data (wavenumbers). The observed wavenumbers showed that the stretching vibrations of tetrahedral site atoms (υ_1-mode) and octahedral site atoms (υ_2-mode) that composed of the samples.

Keywords: $Mg_{0.5}Zn_{0.5-x}Cu_xFe_2O_4$, XRD, SEM, FTIR.

Introduction

Ferrite materials have been under intense research for so long due to their useful electromagnetic characteristics for a large number of applications [Marial, (2013)]. The performance of these materials in their bulk form where the grain dimensions are in micrometer scales is limited to a few megahertz frequency due to their higher electrical conductivity and domain wall resonance [Fawzi, (2010)]. However, the recent technological advances in electronics industry demand even more compact cores for work at higher frequencies. One way to solve this problem is by synthesizing the ferrite particles in nanometric scales before compacting them for sintering. When the size of the magnetic particle is smaller than the critical size for multidomain formation, the particle is in a single domain state. Domain wall resonance is avoided, and the material can work at higher frequencies [IIslam, (1998); Son, (2002)].

This work preferred the Mg based ferrite from the following reasons: it is a slight porous ceramic and the stability of Mg^{2+} ions avoid the appearance of Fe^{2+} ions (essential require to obtain high resistivity) [Pathan, (2010); Patil, (2013)]. In the present work, Copper substituted Magnesium-Zinc ferrites, $Mg_{0.5}Zn_{0.5-x}Cu_xFe_2O_4$ (where x = 0.0 – 0.5 with the step of 0.1) were prepared by solid state reaction method. The as-prepared samples were characterized by XRD, SEM and FTIR spectroscopy to study the structural, microstructural and vibrational characteristics.

[1] Dr, Associate Professor, Department of Physics, University of Computer Studies (Pyay)
[2] Dr, Associate Professor, Department of Physics, Loikaw University
[3] Dr, Assistant Lecturer, Department of Physics, Pyay University
[4] Dr, Associate Professor, Department of Physics, Pyay University

Experimental Details

Preparation of the Samples

Copper substituted Magnesium-Zinc ferrites, $Mg_{0.5}Zn_{0.5-x}Cu_xFe_2O_4$ (where x = 0.0 – 0.5 with the step of 0.1) were prepared by solid state reaction method. Analytical Reagent (AR) grade Magnesium Oxide (MgO), Zinc Oxide (ZnO), Copper Oxide (CuO) and Iron Oxide (Fe_2O_3) were used to prepare the samples. Flow diagram of the sample preparation process is shown in Figure 1.

XRD, SEM and FTIR Measurements

Powder XRD patterns of the samples were observed by RIGAKU MULTIFLEX Powder X-Ray Diffractometer [Universities' Research Centre (URC), University of Yangon]. Microstructural characteristics of the samples were studied by using JEOL JSM-5610LV Scanning Electron Microscope (SEM) [Universities' Research Centre (URC), University of Yangon] with the accelerating voltage of 15 kV, the beam current of 50 mA and 10,000 times of photo magnification. FTIR spectra were observed by PC-controlled FTIR-8400 SHIMADZU Spectrophotometer [Universities' Research Centre (URC), University of Yangon].

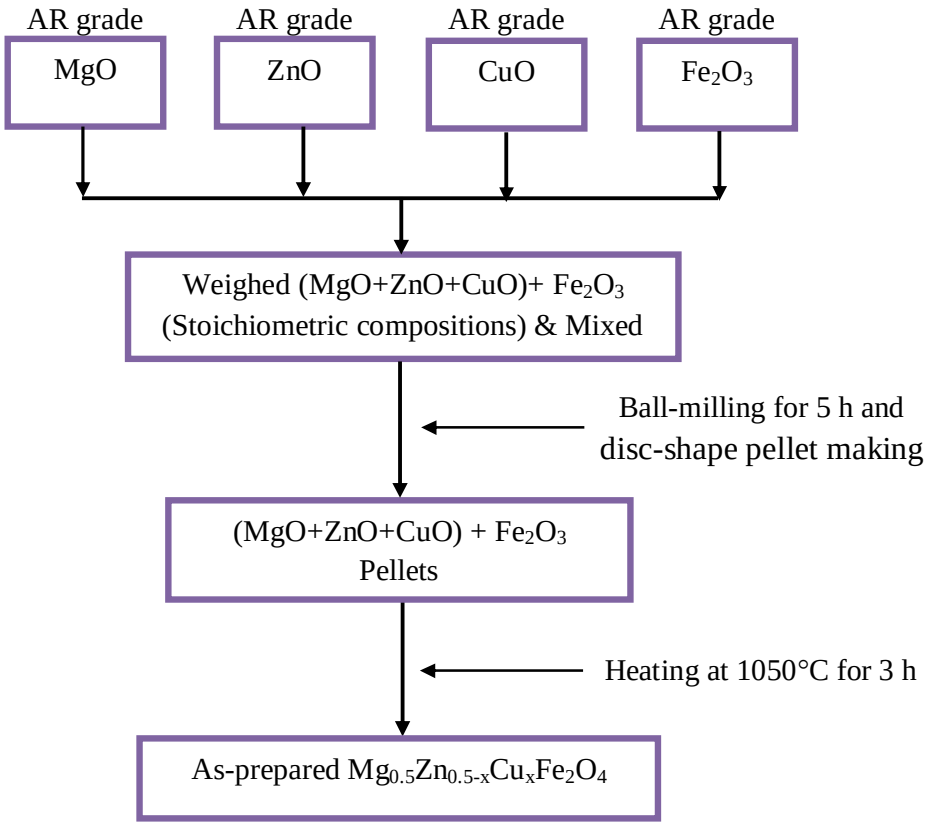

Figure 1 Flow diagram of the sample preparation procedure of $Mg_{0.5}Zn_{0.5-x}Cu_xFe_2O_4$

Results and Discussion

XRD Study

Powder XRD patterns of the samples are shown in Figure 2. The observed diffraction lines were identified by using JCPDS data files. As shown in XRD patterns, most of the collected diffraction lines were assigned with standard JCPDS (Joint Committee on Powder Diffraction Standards) data library files. Some of the lines were not assigned with standard files due to the difference between the standard JCPDS data library files and substitution of materials deviation of diffraction angles of collected lines with standard data files. In the observed XRD patterns, the diffraction line of (311) plane is found to the strongest in intensity (I = 100%) among the diffraction lines.

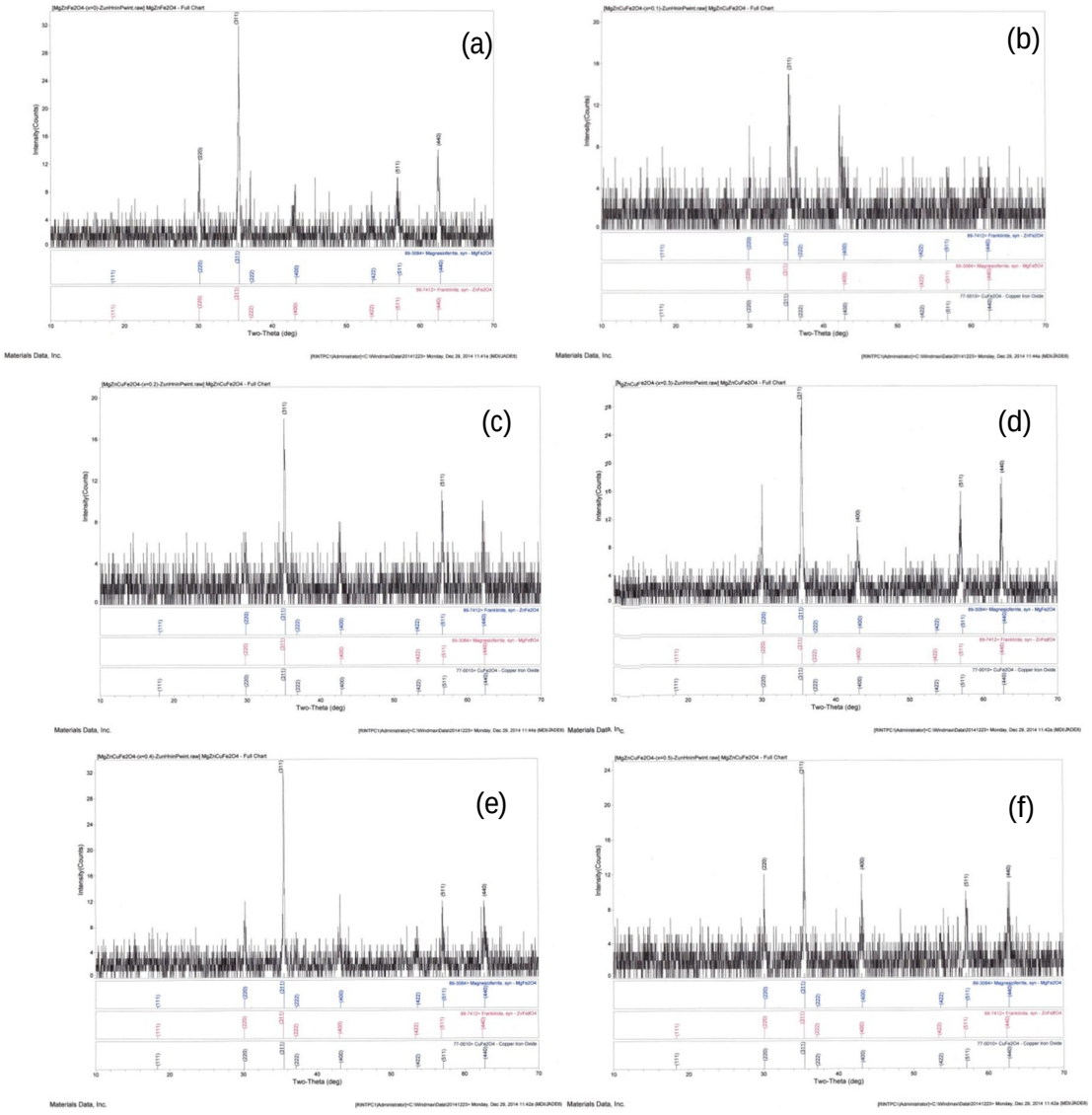

Figure 2 XRD patterns of $Mg_{0.5}Zn_{0.5-x}Cu_xFe_2O_4$ where (a) x = 0.0, (b) x = 0.1, (c) x = 0.2, (d) x = 0.3, (e) x = 0.4 and (f) x = 0.5

XRD patterns indicate the samples belong to cubic structure. For cubic crystals, it is then possible to use $a=\frac{\lambda}{2\sin\theta}\sqrt{h^2+k^2+l^2}$ to convert each interplanar spacing into a lattice parameter, *a*. The indexing is consistent if all peaks provide the same lattice parameter(s). In the present work, the calculated and observed lattice parameters of the samples are tabulated in Table 1. Rezlescu, N. et. al. (2002) has reported that the lattice parameters of the $Mg_{0.5}Zn_{0.5}Fe_2O_4$ or x = 0.00 sample are a = b = c = 8.4060 Å [Rezlescu, (2002)]. In this work, the obtained lattice parameters are compatible with the result of Rezlescu, N. et. al.. The lattice parameters of the samples were varied with increased in concentration of Cu due to the atomic substitution of Cu on Zn in the lattice sites.

The crystallite sizes of the $Mg_{0.5}Zn_{0.5-x}Cu_xFe_2O_4$ samples have been estimated by using the Scherrer formula, $D=\frac{0.9\lambda}{B\cos\theta}$, where *D* is the crystallite size (nm), λ is the wavelength of incident X-ray (Å), θ is diffraction angle of the peak under consideration at

FWHM (°) and B is observed FWHM (radian). In the present work, the average crystallite sizes were calculated and the obtained crystallite sizes are also presented in Table 1. The crystallite sizes of the samples were found to vary with increased in concentration of Cu.

Table 1 The observed and calculated lattice parameters and the crystallite sizes of $Mg_{0.5}Zn_{0.5-x}Cu_xFe_2O_4$

Sample (Contents x of Cu)	Obs. *a=b=c* (Å)	Cal. *a=b=c* (Å)	*D* (nm)
0.0	8.3897	8.3897	52.44
0.1	8.4225	8.4224	86.81
0.2	8.4413	8.4413	108.84
0.3	8.4035	8.4035	44.44
0.4	8.3781	8.3781	40.42
0.5	8.3837	8.3837	92.66

SEM Analysis

Figure 3 shows the SEM micrographs of the samples prepared at 1050°C for 3 h. As shown in SEM micrographs, the grains are small, below 4 μm, and the ceramic bodies are porous. It was found that the grain size ranges from 0.10 μm to 3.20 μm. The porosity within the matrix is relatively cleared. Also, all porosity is distributed along the grain boundaries through the image (except x = 0.5 sample). This structure indicates that the porous ceramic can easily exhibit absorption and condensation of water vapour.

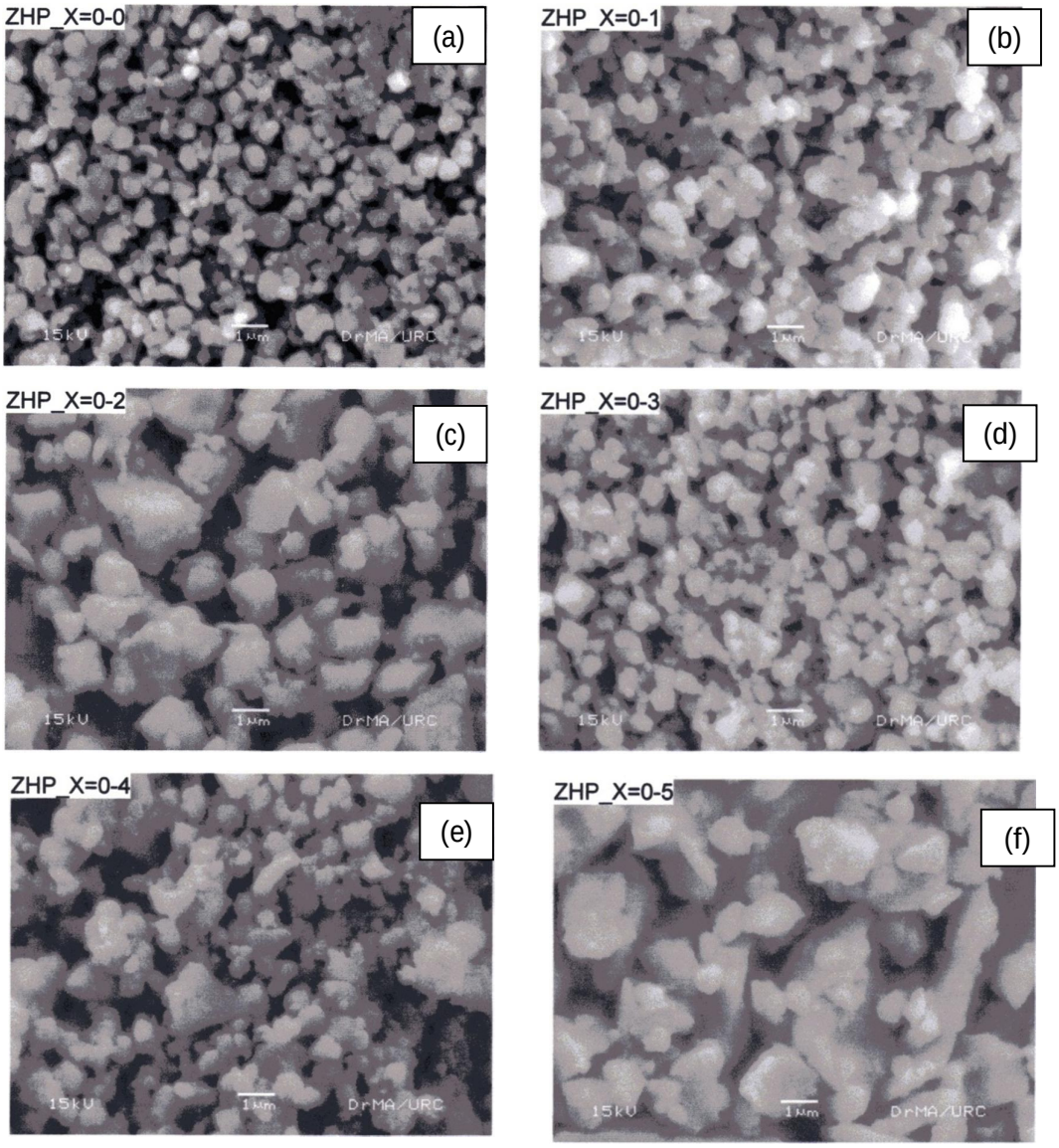

Figure 3 SEM micrographs of $Mg_{0.5}Zn_{0.5-x}Cu_xFe_2O_4$ where (a) x = 0.0, (b) x = 0.1, (c) x = 0.2, (d) x = 0.3, (e) x = 0.4 and (f) x = 0.5

Furthermore, the porous structure is an advantage in discouraging fracture due to thermal shock. The grain shapes were found to be clearly difference in the samples of Cu contents and no-contents. In the most Cu concentration of the sample (x = 0.5), the largest grain size and poor grain boundary. In Figure 3(a), (b), (d) and (e) of x = 0.0, x = 0.1, x = 0.3 and x = 0.4 samples, the grains shapes are nearly spherical but in Figure 3(c) and (f) of x = 0.2 and x = 0.5, the grains shapes are flake. The obtained grain sizes of the samples are tabulated in Table 2. The grain size of the un-substituted (x = 0.0) sample is the smallest one with clearly grain boundary and it is the most homogeneity among the investigated samples.

Table 2 Grain sizes of $Mg_{0.5}Zn_{0.5-x}Cu_xFe_2O_4$

Sample (Contents x of Cu)	Grain size (μm)
0.0	0.10 – 0.80
0.1	0.35 – 1.10
0.2	0.55 – 2.50
0.3	0.25 – 1.20
0.4	0.40 – 1.80
0.5	0.75 – 3.20

FTIR Spectroscopic Analysis

Spinels are generally formulated as AB_2X_4 that formally consider the structure as consisting of isolated ion of B and isolated AX_4 molecules. The so-called normal spinel structure is cubic, space group O_h^7, with eight molecules in the unit cell, and has the B atoms on octahedral sites D_{3d} symmetry, and the A atoms on tetrahedral sites of T_d symmetry. The oxygen atoms occupy C_{3v} sites. The coordination polyhedron around B is a regular octahedron. The vibrational frequencies (wavenumbers) of undoped Zinc Ferrite, $ZnFe_2O_4$, are mainly 550 cm^{-1} and 555 cm^{-1} for A atoms on tetrahedral sites and 415 cm^{-1} for B atoms on octahedral sites. Also, vibrational frequencies of undoped $MgFe_2O_4$ are mainly 565 cm^{-1} and 581 cm^{-1} for A atoms on tetrahedral sites and 406 cm^{-1} and 433 cm^{-1} for B atoms on octahedral sites. Vibrational frequencies of undoped $CuFe_2O_4$ are mainly 592 cm^{-1} for A atoms on tetrahedral sites and 420 cm^{-1} for B atoms on octahedral sites. The frequencies for A-atoms (tetrahedral site) assigned as υ_1-mode and for B-atoms (octahedral site) assigned as υ_2-mode [Ross, (1972)].

In the present work, FTIR transmission spectra of the Copper substituted Magnesium-Zinc ferrites, $Mg_{0.5}Zn_{0.5-x}Cu_xFe_2O_4$ (where x = 0.0 – 0.5 with the step of 0.1) samples are shown in Figure 4. The observed spectral lines (wavenumbers) and the corresponding vibrational mode assignments of molecules are listed in Table 3. Furthermore, the collected wavenumbers and their corresponding vibrational properties (wavelength, frequency, oscillation time and energy) of constituent molecules of the samples are also tabulated in Table 3. As shown in Tables, the obtained data (observed wavenumbers or emitted frequencies with $\bar{\lambda} = \bar{\nu}$ = wavenumbers are found experimentally that the vibrational frequencies of tetrahedral site and octahedral site molecular networks in the samples. The obtained frequencies ($>10^6$ Hz) indicate the samples composed of high frequency oscillators.

As shown in figures, some of the absorption bands observed in the wavenumber ranges of round about 1600 cm^{-1} and 3400 cm^{-1} represent the vibrational characteristics of water (H_2O) and the band observed at about 2300 cm^{-1} represents the vibrational characteristic of carbon dioxide (CO_2) molecules. These two molecules of water and carbon dioxide distributed as the moisture in the atmosphere (surrounding) of FTIR spectrophotometer. Normally, their vibrational modes appeared in a FTIR spectrum of KBr pellet.

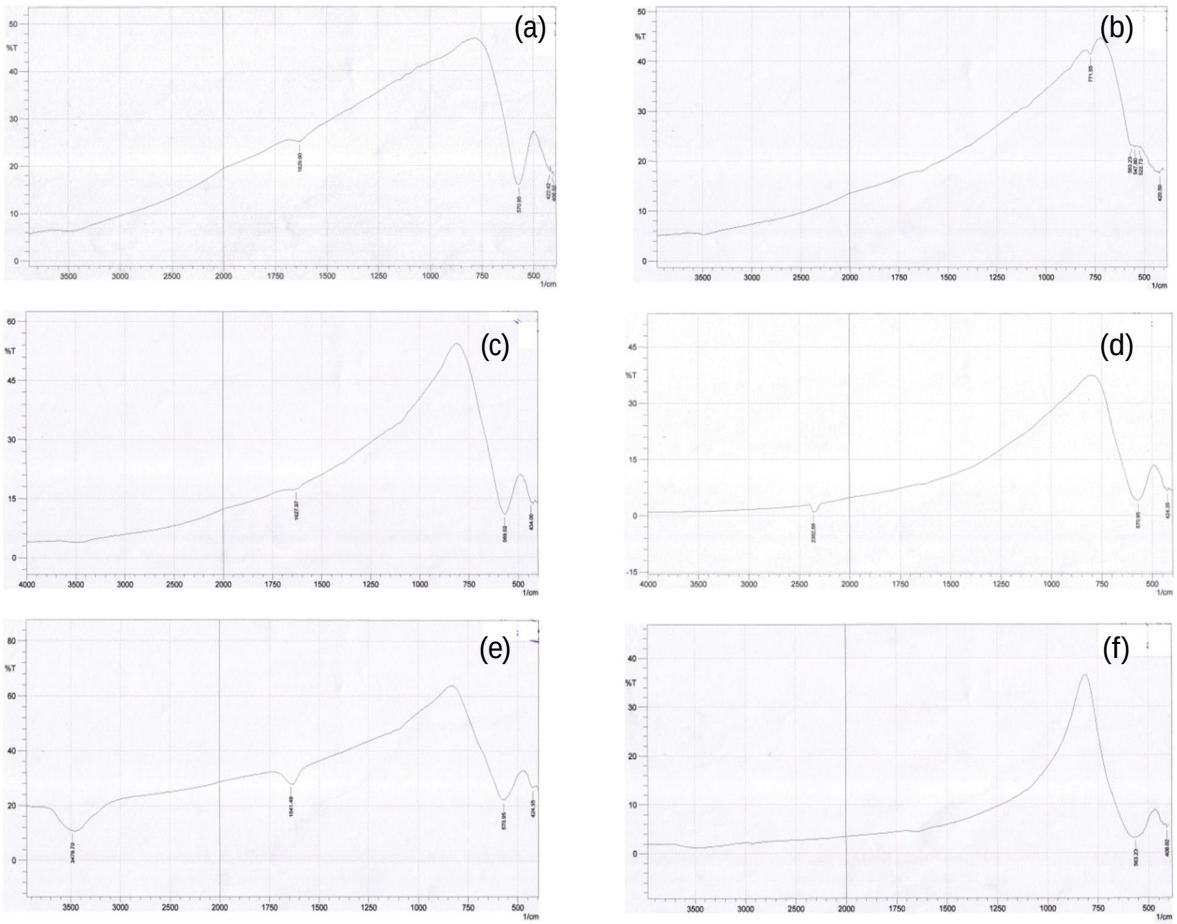

Figure 4 FTIR transmission spectra of $Mg_{0.5}Zn_{0.5-x}Cu_xFe_2O_4$ where (a) x = 0.0, (b) x = 0.1, (c) x = 0.2, (d) x = 0.3, (e) x = 0.4 and (f) x = 0.5

Table 3 (a) Wavenumbers and corresponding vibrational modes and vibrational properties of $Mg_{0.5}Zn_{0.5-x}Cu_xFe_2O_4$ (where x = 0.0)

$\bar{\nu}$ (1/cm)	Mode	Molecule	λ(nm)	υ (Hz)	τ (s)	E(eV)
409, 422	υ_2-mode (stretching)	B atoms on octahedral site	24450, 23697	1.226E+13, 1.265E+13	8.156E-14, 7.904E-14	0.0508, 0.0524
571	υ_1-mode (stretching)	A atoms on tetrahedral site	17513	1.712E+13	5.842E-14	0.0709

Table 3. (b) Wavenumbers and corresponding vibrational modes and vibrational properties of $Mg_{0.5}Zn_{0.5-x}Cu_xFe_2O_4$ (where x = 0.1)

$\bar{\nu}$ (1/cm)	Mode	Molecule	λ(nm)	υ (Hz)	τ (s)	E(eV)
421	υ_2-mode (stretching)	B atoms on octahedral site	23753	1.262E+13	7.923E-14	0.0523
523, 548, 563	υ_1-mode (stretching)	A atoms on tetrahedral site	19120, 18248, 17762	1.568E+13, 1.643E+13, 1.688E+13	6.378E-14, 6.087E-14, 5.924E-14	0.0649, 0.0680, 0.0699
772	υ-Combination	A atoms +B atoms	12953	2.314E+13	4.321E-14	0.0958

Table 3 (c) Wavenumbers and corresponding vibrational modes and vibrational properties of $Mg_{0.5}Zn_{0.5-x}Cu_xFe_2O_4$ (where x = 0.2)

$\bar{\nu}$ (1/cm)	Mode	Molecule	λ(nm)	υ (Hz)	τ (s)	E(eV)
434	υ_2-mode (stretching)	B atoms on octahedral site	23041	1.301E+13	7.686E-14	0.0539
569	υ_1-mode (stretching)	A atoms on tetrahedral site	17575	1.706E+13	5.862E-14	0.0706
1628	υ_2-mode (bending)	H_2O	-	-	-	-

Table 3 (d) Wavenumbers and corresponding vibrational modes and vibrational properties of $Mg_{0.5}Zn_{0.5-x}Cu_xFe_2O_4$ (where x = 0.3)

$\bar{\nu}$ (1/cm)	**Mode**	**Molecule**	**λ(nm)**	**υ (Hz)**	**τ (s)**	**E(eV)**
424	υ_2-mode (stretching)	B atoms on octahedral site	23585	1.271E+13	7.867E-14	0.0526
571	υ_1-mode (stretching)	A atoms on tetrahedral site	17513	1.712E+13	5.842E-14	0.0709
2363	υ_2-mode (bending)	CO_2	-	-	-	-

Table 3 (e) Wavenumbers and corresponding vibrational modes and vibrational properties of $Mg_{0.5}Zn_{0.5-x}Cu_xFe_2O_4$ (where x = 0.4)

$\bar{\nu}$ (1/cm)	**Mode**	**Molecule**	**λ(nm)**	**υ (Hz)**	**τ (s)**	**E(eV)**
424	υ_2-mode (stretching)	B atoms on octahedral site	23585	1.271E+13	7.867E-14	0.0526
571	υ_1-mode (stretching)	A atoms on tetrahedral site	17513	1.712E+13	5.842E-14	0.0709
1641	υ_2-mode (bending)	H_2O	-	-	-	-
3480	υ_3-mode (asymmetric-stretching)	H_2O	-	-	-	-

Table 3. (f) Wavenumbers and corresponding vibrational modes and vibrational properties of $Mg_{0.5}Zn_{0.5-x}Cu_xFe_2O_4$ (where x = 0.5)

$\bar{\nu}$ (1/cm)	**Mode**	**Molecule**	**λ (nm)**	**υ (Hz)**	**τ (s)**	**E (eV)**
409	υ_2-mode (stretching)	B atoms on octahedral site	24450	1.226E+13	8.156E-14	0.0508
563	υ_1-mode (stretching)	A atoms on tetrahedral site	17762	1.688E+13	5.924E-14	0.0699

Conclusion

Copper substituted Magnesium-Zinc ferrites, $Mg_{0.5}Zn_{0.5-x}Cu_xFe_2O_4$ (where x = 0.0, 0.1, 0.2, 0.3, 0.4 and 0.5) were prepared by solid-state reaction method. Structural, microstructural and vibrational characteristics of the samples were reported by XRD, SEM and FTIR spectroscopic methods. XRD patterns showed that the samples analogous to cubic structure. The lattice parameters and the crystallite sizes of the as-prepared samples were varied with increase in concentration of Cu on the atomic sites of Zn. SEM micrographs showed that the grain shape and size were generally varied with the concentration of Cu in the samples. Some pores appeared in the observed SEM micrographs and they showed that the sample may be sensitive material for the application of environmental effect sensors, such as humidity and gas sensors. According to FTIR spectra, the υ_1-mode of tetrahedral site atoms and the υ_2-mode of octahedral site atoms were appeared and assigned by using standard wavenumbers. The appearance of the lines in the FTIR spectra showed that the vibrational characteristics of the samples. It showed that phase formation of the samples was valid or the phase formation from the XRD results well confirmed by FTIR spectroscopy.

Acknowledgement

The authors would like to acknowledge Professor Dr Khin Khin Win, Head of Department of Physics, University of Yangon, for her valuable suggestion and comments for this work.

References

Fawzi, A.Z., A.D. Sheikh, & V.L. Mathe, (2010) "Structural, Dielectric Properties and AC Conductivity of $Ni_{(1-x)}Zn_xFe_2O_4$ Spinel Ferrite." *Journal of Alloys and Compounds*, vol. 502, pp. 231-237.

IIslam, M.U., M.U. Rana, & Abbas, (1998) "Study of Magnetic Interactions in Co-Zn-Fe-O System." *Materials Chemistry and Physics*, vol. 57, pp. 190-193.

Maria1, K.H., S. Choudhury, & M.A. Hakim, (2013) "Structural Phase Transformation and Hysteresis Behavior of Cu-Zn Ferrites." *International Nano Letters*, vol. 3, pp. 2-10.

Pathan, A.N., K. Sangshetti, & A.A.G. Pangal, (2010) "Synthesis and Moussbauer Studies on Nickel-Zinc-Copper Nanoferrites." *Nanotechnology and Nanoscience*, vol. 1, pp. 13-16.

Patil, S.N., & B.P. Ladgaonkar, (2013) "Synthesis and Implementation of $NiZnFe_2O_4$ Ferrites to Design Embedded System for Humidity Measurement." *International Journal of Advanced Research in Electrical, Electronics and Instrumentation Engineering*, vol. 2, pp. 3813-3821.

Rezlescu, N., E. Rezlescu, P. Popa, & F. Tudorache, (2002) "On the Humidity Sensitivity of a Ceramic Element. Structure and Characteristics." *Journal of Institute of Technical Physics*, vol. 8, pp. 89-97.

Ross, S.D., (1972) *Inorganic Infrared and Raman Spectra*. London, McGraw-Hill.

Son, S., & M. Taheri, (2002) "Synthesis of Ferrite and Nickel Ferrite Nanoparticles Using Radio-Frequency Thermal Plasma Torch." *Journal Apply Physics*, vol. 91, pp. 7589-7591.